Slurry Reactor Studies of Homogeneous and Heterogeneous Reactions

A dynamic model is derived for simultaneous, homogeneous and heterogeneous, first-order reactions in a slurry reactor. The theory is applied to experimental data for the oxidation (with gaseous oxygen) of aqueous sulfite solutions which is first order in oxygen and zero order in sulfite. The homogeneous reaction is very slow at low pH (2-3) where the sulfur exists as dissolved SO_2 or HSO_3^-, even when cobalt is added as a homogeneous catalyst. At higher pH (7-8.5), considerable homogeneous reaction occurs with and without cobalt ions. Here the predominant species are $SO_3^=$ and HSO_3^-. Activated carbon is not a heterogeneous catalyst at pH 7 or 8.5, but is responsible for nearly all the reaction at the low pH values. Analysis of the heterogeneous data indicates that the surface reaction between adsorbed oxygen and SO_2 controls the rate rather than adsorption of oxygen.

Chen-Chen Fu
B. J. McCoy
J. M. Smith
Department of Chemical Engineering
University of California
Davis, CA 95616

Introduction

Reactions often occur both homogeneously and with a heterogeneous catalyst. Examples are liquid-phase oxidation of aromatic hydrocarbons using metal catalysts (Gould and Rado, 1969; Newberg et al., 1972; Taylor, 1970; Vreugdenhil, 1973). The homogeneous reaction may be thermal or catalytic. Aqueous sulfite ions are oxidized without a catalyst (Yago and Inoue, 1962) but also cobalt ions are an excellent homogeneous catalyst (de Waal and Okeson, 1966).

The first objective of this research was to develop a dynamic model for simultaneous homogeneous and heterogeneous catalytic reaction in a well-mixed slurry reactor. Chaudari and Ramachandran (1980) have presented a mathematical model for such simultaneous reaction in a slurry reactor operating at steady state. At steady state, only the overall reaction rate can be determined from experimental measurements. With dynamic data, it is possible to establish rates of the individual steps which constitute overall catalytic reaction (Ahn et al., 1986; Recasens et al., 1984; Fu, et al., 1988; Muller and Hoffmann, 1987a, b; Kaul et al., 1987). In the dynamic model given here, all steps are first order so that the moment method of analysis is applicable.

The second objective was to test the dynamic theory with experiments for the homogeneous and heterogeneous (activated carbon catalyst) oxidation of aqueous sulfite solutions at 295 K and 101 kPa. At the concentrations employed both the homogeneous and heterogeneous reactions are first order in oxygen and zero order in sulfite (Komiyama and Smith, 1975; Fu et al., 1988). The procedure was to introduce a pulse of reactant oxygen into a stirred solution of sodium sulfite with carbon particles and to measure the oxygen concentration in the gas stream leaving the reactor (i.e., monitor the response curve). In some experiments, cobalt sulfate was added as a homogeneous catalyst.

It was found that activated carbon was not catalytically active at pH 7 or 8.5, but that the homogeneous reaction with or without cobalt ions as a catalyst resulted in considerable conversion. At pH 2 or 3, carbon was an active catalyst while the homogeneous reaction with or without cobalt occurred only to a small extent. Analysis of the data for the heterogeneous reaction indicated that surface reaction of adsorbed oxygen and sulfur dioxide controlled the overall rate rather than the adsorption step. From equilibrium calculations for the sulfur-containing components, $SO_3^=$ and HSO_3^- were the only species present at pH = 7 to 8.5, and only dissolved and adsorbed SO_2 molecules and HSO_3^- at pH 2–3. This information suggested that $SO_3^=$ and HSO_3^- were the only possible reactive species at high pH, and SO_2 molecules and HSO_3^- at low pH.

Theory

The development is for the homogeneous reaction in the "slow regime," i.e., reaction occurs predominantly in the bulk liquid rather than in the thin liquid film surrounding the gas bubbles. The conditions for the experimental work are the same as in the earlier study of Fu et al. (1988) where the reaction was

assumed to occur in the bulk liquid. No intraparticle diffusion resistance is included. Small carbon particles were used (Table 1) so that the effectiveness factor was nearly unity, as found for the same reaction by Ahn et al. (1986) and Recasens et al. (1984). Other restrictions are isothermal operation, spherical particles, and well-mixed slurry and gas bubbles. For the heterogeneous path a two-step mechanism is employed: first-order reversible adsorption of oxygen on the catalyst surface followed by an irreversible first-order surface reaction. The homogeneous reaction is assumed to occur by a single, first-order irreversible step.

For the homogeneous reaction (high pH) SO_3^- is the predominant species. Hence, the reaction may be written in overall form as

$$2\,SO_3^-(aq) + O_2(g) \rightarrow 2\,SO_4^-$$

The carbon-catalyzed, two-step reaction at low pH may be written

$$O_2(g) + M \rightleftharpoons O_2 \cdot M$$

$$O_2 \cdot M + 2\,SO_2 \rightarrow 2\,SO_3 \cdot M$$

where M is the carbon catalyst, $O_2 \cdot M$ the absorbed oxygen, and $SO_3 \cdot M$, the adsorbed SO_3, is desorbed rapidly into the solution, forming H_2SO_4. It should be emphasized that these reactions do not necessarily represent the actual reaction mechanisms but simply reflect the observed kinetics of oxygen for the homogeneous and heterogeneous reactions.

Basic equations

With the mentioned postulates mass conservation equations for the reactant in the gas bubbles, slurry liquid, liquid-filled pores of the catalyst particles, and at the adsorption-reaction site are

$$V_B V_L \frac{dC_g}{dt} = Q\,(C_{go} - C_g) - k_L a_B V_L \left(\frac{C_g}{H} - C_L\right) \tag{1}$$

$$\left(1 - \frac{\beta m_s}{\rho_p}\right)\frac{dC_L}{dt} = k_L a_B \left(\frac{C_g}{H} - C_L\right) - k_s a_s\,(C_L - C_i) - \left(1 - \frac{\beta m_s}{\rho_p}\right) k_t C_L \tag{2}$$

$$\beta \frac{dC_i}{dt} = \frac{3}{R} k_s\,(C_L - C_i) - \rho_p k_o \left(C_i - \frac{n}{K}\right) - \beta k_t\, C_i \tag{3}$$

Table 1. Properties of BPL Activated Carbon*

Parameters	Properties
Surface area (N_2, BET method), m^2/kg	1.05×10^6 to 1.15×10^6
Solid density, kg/m^3	2.1×10^3
Particle density ρ_p, kg/m^3	0.85×10^3
Porosity, β	0.60
Avg. particle dia. (150–250 mesh), μm	82.5
Mean pore radius in particles, nm	1.3

*From data sheet, Calgon Corp., Pittsburgh, PA 15230

$$\frac{dn}{dt} = k_a \left(C_i - \frac{n}{K}\right) - k_r n \tag{4}$$

where C_g, C_L, C_i, and n are concentrations of reactant (oxygen) in the gas, bulk liquid, liquid in pores, and adsorbed on the pore surface. The term $(1 - \beta m_s/\rho_p)\, k_t C_L$ is the rate of reaction in the bulk liquid (excluding liquid inside particle pores), and $\beta k_t C_i$ is the rate of homogeneous reaction inside the pores.

The initial conditions are

$$C_g = C_L = C_i = n = 0 \qquad \text{at } t = 0 \tag{5}$$

and the input to the system is an impulse function,

$$C_{go} = A\delta(t) \tag{6}$$

The moments of the response curve in the gas effluent can be expressed in terms of the solution in the Laplace domain without inverting the transform. The necessary relation is

$$m_n = (-1)^n \lim_{s \to 0} \frac{d^n \bar{C}_g(s)}{ds^n} \tag{7}$$

where $\bar{C}_g$ is the Laplace transform of C_g.

After solution of Eqs. 1 to 6 in the Laplace domain, the normalized zero and first temporal moments are obtained from Eq. 7. The results are

$$m_o = \left[1 + K_L - \frac{K_L}{1 + B_o}\right]^{-1} \tag{8}$$

$$m_1 = \frac{\dfrac{V_o V_L}{Q}(1 + B_o)^2 + K_L(\epsilon + B_s)}{[1 + B_o + K_L B_o]^2} \tag{9}$$

The dimensional groups are defined as

$$B_s = \frac{Ra_s}{3k_L a_B}\left[\frac{1}{\left(1 + \dfrac{R\rho_p k_o}{3k_s}\right)^2}\right]\left[\beta + \frac{\rho_p k_o}{\left(1 + \dfrac{Kk_r}{k_a}\right)^2}\right] \tag{10}$$

$$\epsilon = \frac{\left(1 - \dfrac{\beta m_s}{\rho_p}\right)}{k_L a_B} \tag{11}$$

$$k_o = \frac{\beta}{\rho_p} k_t + k_p \tag{12}$$

$$k_p = \frac{Kk_r k_a}{Kk_r + k_a} \tag{13}$$

and the dimensionless groups are

$$B_o = \frac{1}{k_L a_B}\left[\left(1 - \frac{\beta m_s}{\rho_p}\right) k_t + k_s a_s \left(\frac{R\rho_p k_o}{R\rho_p k_o + 3k_s}\right)\right] \tag{14}$$

$$K_L = \frac{k_L a_B V_L}{QH} \tag{15}$$

Experimental values of the moments are obtained from the measured response curves, for the pulse input, from the equations

$$m_o = \int_0^\infty C_g dt \Big/ \int_0^\infty C_{go} dt \tag{16}$$

$$m_1 = \int_0^\infty tC_g dt \Big/ \int_0^\infty C_{go} dt \tag{17}$$

Equating predicted (Eqs. 8 and 9) and experimental moments provides the means for evaluating the rate parameters.

Method of analysis

The zero moment is equivalent to the unreacted fraction of the reactant so that $1 - m_o$ is the conversion x. Therefore, Eq. 8 with the expression for B_o (Eq. 14) can be expressed in terms of conversion as:

$$\frac{1}{x} = \frac{1}{1 - m_o} = \left(1 + \frac{1}{K_L}\right) + \frac{QH}{V_L}\left[\left(1 - \frac{\beta m_s}{\rho_p}\right) k_t + k_s a_s \left(\frac{R\rho_p k_o}{R\rho_p k_o + 3k_s}\right)\right]^{-1} \tag{18}$$

where for spherical particles,

$$a_s = \frac{3m_s}{R\rho_p} \tag{19}$$

The dimensionless group K_L is independent of Q, since both a_B and V_B in Eq. 15 are proportional to Q. The requirement for this linearity is that the bubble size does not change with gas flow rate. The bubble diameter as measured by Misic and Smith (1971), over a range of Q values similar to those used in our experiment with a similar dispersion tube, did not change significantly.

With K_L independent of Q, Eq. 18 shows that a straight line should result by plotting $(1 - m_o)^{-1}$ vs. QH/V_L. The slope of this line gives k_o and from Eq. 12 the rate constant k_p for the heterogeneous catalyst, provided k_t and $k_s a_s$ are known. The homogeneous rate constant, k_t, can be obtained from experiments without the heterogeneous catalyst. This rate constant in general would include the total catalytic plus noncatalytic rates. When there is no homogeneous catalyst, $k_t = k_h$. For this situation m_s and a_s are zero, and the only rate constant in the bracketed term in Eq. 18 is k_t. Hence, the slope of the line described by such data establishes k_t. While not necessary for evaluating the reaction rate constants, the intercept of the linear plots determines K_L and from it the gas bubble-to-liquid mass transfer coefficient $k_L a_B$.

The measured first moments include the residence time in the dead volume (V_d). Thus the observed, reduced first moment can be expressed as

$$\mu_1^o = \frac{m_1}{m_o} + \frac{V_d}{Q} \tag{20}$$

Since $V_d = V_o - V_B V_L$, Eq. 8 for m_o and Eq. 9 for m_1 can be used to rewrite Eq. 20 as

$$\mu_1^o\left(\frac{Q}{V_L}\right) + V_B(1 - m_o) = \left(1 - \frac{\beta m_s}{\rho_p}\right) + m_s\left\{\left[\frac{1}{\left(1 + \frac{R\rho_p k_s}{3k_s}\right)^2}\right]\left[\frac{\beta}{\rho_p} + \frac{K}{\left(1 + \frac{Kk_r}{k_a}\right)^2}\right]\right\} \times \frac{m_o}{H}\left(1 + \frac{1}{K_L} - \frac{1}{m_o K_L}\right)^2 + \frac{V_o}{V_L} \tag{21}$$

where V_o is the dead volume without gas flow through the reactor. Due to the small gas holdup, V_B, in the slurry reactor, the term $V_B(1 - m_o)$ can be neglected (Ahn et al., 1986). Then a straight line is expected if the known left side of Eq. 21 is plotted vs. $m_o/H\,[1 + (1/K_L) - (1/m_o K_L)]^2$. The slope of such a line yields a value of the ratio Kk_r/k_a. This ratio along with the k_p results and Eq. 13 provides two relationships for k_a and k_r.

To determine k_a and k_r separately, the adsorption equilibrium constant must be known. While it could, in principle be calculated from second moments of the response data, these values are not sufficiently accurate. Hence, K is obtained best from the first moments for oxygen adsorption runs, i.e., in the absence of reaction in both homogeneous and heterogeneous phases. Under this condition, Eq. 21 reduces to

$$\mu_1^o = \frac{V_L}{Q}\left[\frac{1 + m_s K}{H} + \frac{V_o}{V_L}\right] \tag{22}$$

which shows that the slope of a plot of μ_1^o vs. V_L/Q yields K when H and V_o are known.

Experimental

Figure 1 is a schematic diagram of the slurry reactor and apparatus for the pulse-response measurements. Helium carrier gas flowed continuously through the reactor from cylinder. A seven-port valve equipped with a 5×10^{-6} m^3 sample loop was used to introduce a pulse of pure oxygen into the reactor via dispersion tube. The cylindrical Pyrex reactor, about 0.15 m long and 0.10 m diameter, contained an eight-bladed Teflon impeller operated at 8.8 rps and eight lucite buffles. The entire reactor

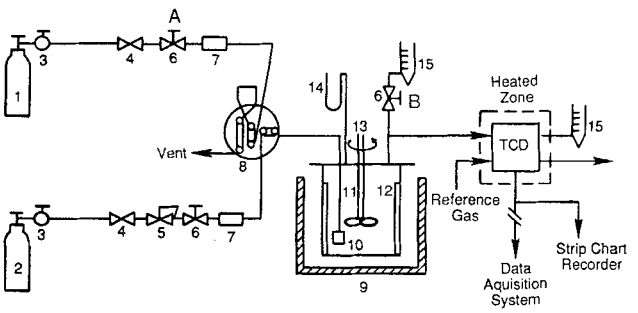

1. Sample Gas, O_2
2. Carrier Gas, He
3. Pressure Regulator
4. Shut Off Valve
5. Flow Regulator
6. Needle Valve
7. Rotameter
8. 7 Port Sample Valve
9. Constant Temperature Bath
10. Gas Sparger
11. Stirrer
12. Baffle
13. Reactor
14. Mercury Manometer
15. Soap Bubble Meter

Figure 1. Apparatus.

assembly was immersed in a constant temperature water bath maintained at 295 K. Complete details of the reactor and accessories are available (Fu, 1988).

A constant flow rate of 9.3×10^{-6} m^3/s of effluent gas from the reactor was passed through the thermal conductivity detector (TCD) and the remainder of the stream measured with a precision soap-film meter before discharge. The analog response from the TCD was transmitted via an A/D converter (Scientific Solution Company, Model TM-40-PRK) to an IBM personal computer for calculation of the moments for the oxygen concentration.

The heterogeneous catalyst was type BPL activated carbon (from Calgon Corp.). It was crushed and sieved, retaining particles between 150 and 250 mesh screens (average diameter = 82.5 μm). Prior to use the particles were dried at 423 K for four hours to remove adsorbed gases. Then they were weighed and immediately added to the solution in the reactor. Physical properties of the carbon are given in Table 1.

The aqueous sulfite solution (0.25 kmol/m^3) was prepared from analytical grade sodium sulfite and distilled water. The pH of the solution was monitored with a pH meter and adjusted to the chosen values by adding drops of 4 normal H_2SO_4 solution.

The operating procedure was, first, to purge the system for one hour with helium. Then pulses of oxygen were introduced and response curves measured over a fivefold range of gas flow rate. Runs were made at pH levels of 2, 3, 7 and 8.5 with and without carbon particles in order to obtain data for both the homogeneous and heterogeneous reactions. The adsorption equilibrium constant for oxygen on activated carbon was determined at pH of 6 and 9 from experiments using only distilled water as the slurry liquid.

Because gaseous SO_2 evolved from the reactor at low pH, TCD measurements of homogeneous oxidation of sulfite ion were conducted using a step input. The apparatus for the step-response experiments is similar to that used by Recasens et al. (1984). To avoid large consumption of the liquid reactant in the reactor, oxygen for step input measurements was diluted by mixing with inert gas He in a feed tank (10% O_2 and 90% He). A four-way valve was used to introduce a step function of the feed gas mixture. After removal of most of the water vapor in an ice trap, a seven-port sample valve with a 0.25×10^{-6}m^3 sample loop was used to introduce at 0.5 min intervals a sample to a gas chromatograph for determination of oxygen concentration. A Porapak-N column (1 m long) at 333 K gave a good separation of SO_2 and O_2 with an analysis time of about 2 minutes. For the experiments with carbon particles at low pH, the SO_2 adsorbs strongly to the high surface area carbon particles and cannot be stripped out of solution in detectable amounts.

There were significant amounts of homogeneous reaction without a catalyst at pH 7 and 8.5 but not at pH 2 or 3. Also, it was known (Fu et al., 1988) that cobalt ions were an effective homogeneous catalyst at high pH in a concentration of 5.64×10^{-2} kg/m^3. To test cobalt activity at low pH, runs were made at pH = 3 in a sulfite solution containing $CoSO_4$ at the same concentration. No carbon was used in these runs. Operating conditions are summarized in Table 2.

Table 2. Operating Conditions

Parameters		Conditions
Reactor volume, m^3		1.255×10^{-3}
Impeller speed, rps		8.8
Temperature, K		295
Reactor pressure		Atmospheric
Volume of sulfite soln., m^3		1.05×10^{-3}
Gas flow rates (1 atm, 298 K), m^3/s		1.0×10^{-6} to 5.0×10^{-6}
	Homogeneous Oxidation Reaction	Combined Homogeneous and Heterogeneous Oxidation Reaction
Cat. conc., kg/m^3	5.64×10^{-2} ($CoSO_4$ at pH = 3 only)	143 (carbon)
pH	3, 7, 8.5	2, 3, 7, 8.5

Results

Figure 2 shows zero moment data for pH 7 and 8.5 plotted as $(1 - m_o)^{-1}$ vs. QH/V_L. Since Henry's constant H for oxygen in the sulfite solution could not be measured directly because of reaction, it was calculated from van Krevelen's correlation (van Krevelen and Hoftijzer, 1948) for 0.25 kmol/m^3 Na_2SO_4 solution. By this method $H = 38.5$ at 295 K.

Data are given in Figure 2 both with and without the carbon particles. The results indicate that at pH 7 or 8.5 activated carbon has no activity, but at these pH levels cobalt ions are an effective homogeneous catalyst. This is indicated by the dotted line (from Fu et al., 1988) which corresponds to oxidation in a solution containing 5.64×10^{-2} kg/m^3 of $CoSO_4$.

The zero-moment data for pH = 2 and 3 are shown in Figure 3. The upper two sets of data for which no carbon has been added show that cobalt ions are not active as a homogeneous catalyst at these pH levels. The cobalt concentration was the same as in Figure 2 where at pH of 8.5 cobalt ions were very effective.

The lower sets of data in Figure 3 are for runs with activated carbon at the same concentrations as in Figure 2. High conversions are obtained indicating that carbon is an effective heterogeneous catalyst at low pH.

Homogeneous and heterogeneous reactants

These contrasting effects of pH on the catalytic activities of cobalt ions and activated carbon can be clarified in part by examining the concentrations of SO_3^-, HSO_3^- and dissolved SO_2 as a function of pH. If equilibrium is assumed between

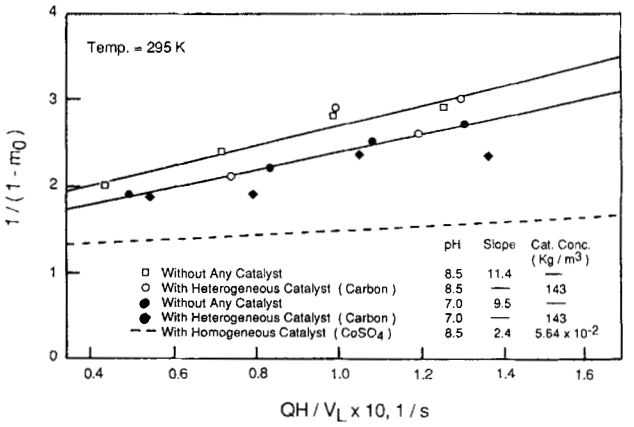

Figure 2. Zero moments for homogeneous and heterogeneous oxidation of sulfite (pH = 7 and 8.5).

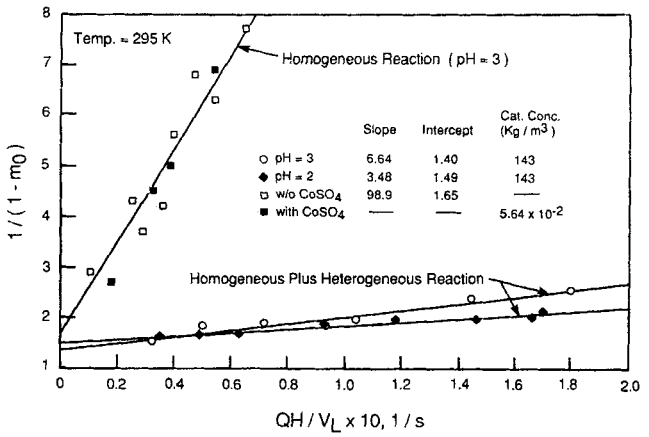

Figure 3. Zero moments for homogeneous and heterogeneous oxidation of SO_2 (pH = 2 and 3).

these species, the concentrations can be calculated from the following equilibrium constant data at 298 K (Skoog and West, 1976):

$$\frac{[H^+]\,[SO_3^=]}{[HSO_3^-]} = 6.43 \times 10^{-8}\ \text{kmol/m}^3 \qquad (23)$$

$$\frac{[H^+]\,[HSO_3^-]}{[SO_2]} = 1.72 \times 10^{-2}\ \text{kmol/m}^3 \qquad (24)$$

and the sulfur mass balance in the 0.25 kmol/m^3 Na_2SO_3 solution

$$0.25 = [SO_3^=] + [HSO_3^-] + [SO_2] \qquad (25)$$

The resulting concentration profiles, Figure 4, show that SO_2 and $SO_3^=$ do not coexist, but that HSO_3^- is present over a wide range of hydrogen ion concentrations. These concentrations indicate that the reactive sulfur species for the homogeneous reaction at pH levels of 7 and 8.5 could be $SO_3^=$ and/or HSO_3^-. The reactivity of HSO_3^- is not clear. Boyce et al. (1984) studied sulfite oxidation with cobalt catalyst and found no reaction at pH = 4.4 where HSO_3^- is the only species present. When the pH was increased to 6.9 a significant oxidation rate occurred, leading the authors to conclude that $SO_3^=$ rather than HSO_3^- was the dominant reactive species. Chang et al. (1987), with initial pH values of 3.5 to 4 where HSO_3^- is the dominant species, found significant reaction without a homogeneous catalyst. All that can be concluded from our work is that: 1) $SO_3^=$ and HSO_3^- are the only possible reactants at pH of 7 and 8.5, and 2) at pH of 3, the small amount of homogeneous reaction (Figure 3) occurs with HSO_3^- or dissolved SO_2. Chang et al. (1987) found evidence that HSO_3^- was oxidized by first forming the intermediate disulfate ion $S_2O_7^=$ which then decayed into sulfate and hydrogen ions.

To evaluate the active sulfur species for the heterogeneous reaction, concentration profiles were recalculated taking into account the adsorption of SO_2 on the activated carbon. It is known that oxygen adsorption is small (Komiyama and Smith, 1975). Adsorption of $SO_3^=$ and HSO_3^- was neglected in these calculations. Then Eq. 25 becomes

$$0.25 = [SO_3^=] + [HSO_3^-] + [SO_2] + [SO_2]_A \qquad (26)$$

The adsorbed sulfur dioxide concentration $[SO_2]_A$ in kmol/m^3 of solution, assuming equilibrium, is given by the Freundlich isotherm at 298 K, as measured by Komiyama and Smith (1975):

$$[SO_2]_A = 4.56 \times 10^{-3}\, m_s\, [SO_2]^{0.532} \qquad (27)$$

The resulting concentrations are shown in Figure 5 for the carbon concentration used in our reaction studies. It is well known that activated carbon is an active catalyst for SO_2 oxidation (Hartman et al., 1971). Hence the high conversions of oxygen at low pH seen in Figure 3 are expected since adsorbed SO_2 concentrations are large (Figure 5). Bisulfite ions and dissolved SO_2, also present at low pH, are not as important reactants as seen from the low conversions shown in Figure 3, with or without homogeneous catalyst. Hence, at low pH the dominant reaction is heterogeneous with adsorbed SO_2 as the reacting sulfur species. Figure 2 shows that at high pH, carbon is not active catalytically since essentially the same conversions were observed with and without carbon. This means that $SO_3^=$ or HSO_3^- oxidation is not affected by carbon.

At low pH some dissolved SO_2 is stripped from the liquid into the gas phase, since SO_2 is the major sulfur species (Figure 5). However, this does not influence the results of the research

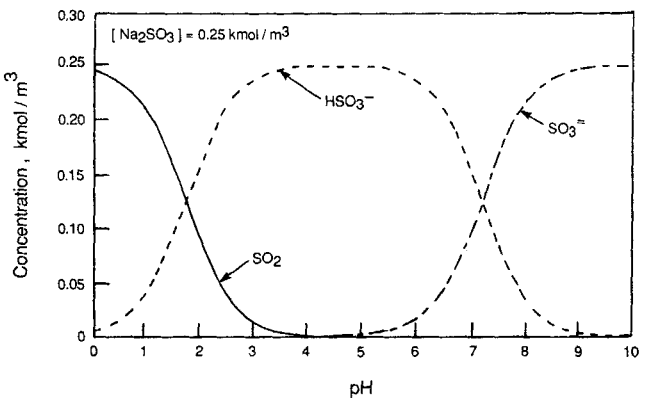

Figure 4. Concentrations of SO_2, HSO_3^-, and $SO_3^=$ in solution at different pH.

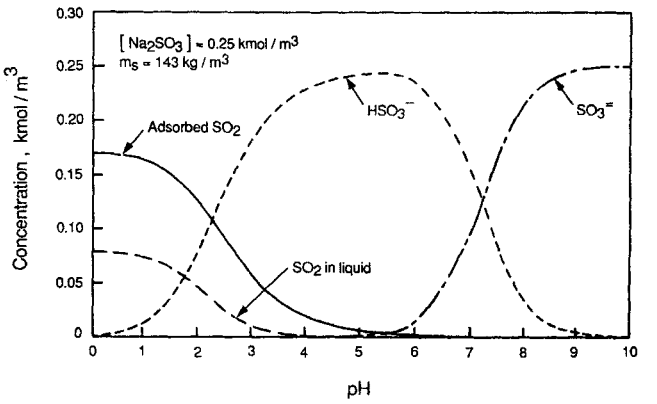

Figure 5. Concentrations of adsorbed SO_2 and SO_2, HSO_3^- and $SO_3^=$ in solution at different pH.

because initially a large excess of Na_2SO_3 is added and because the reaction rate is zero order in SO_2. As noted, only the carbon-catalyzed reaction is significant at low pH. Furthermore, the SO_2 transferred into the gas causes the equilibrium between $SO_3^=$, HSO_3^- and dissolved SO_2 to be reestablished. Thus, the SO_2 concentration in the liquid and adsorbed to carbon tends to increase back toward its initial value.

Homogeneous rate constants (bulk liquid values)

With m_s and $k_s a_s$ zero, Eq. 18 becomes

$$\frac{1}{1 - m_o} = \left(1 + \frac{1}{K_L}\right) + \frac{QH}{V_L} k_h \tag{28}$$

Hence, the slopes of the lines in Figures 2 and 3 for the homogeneous reaction are equal to k_h. Table 3 shows the results at pH of 3, 7 and 8.5. The accuracy of the data are such that the difference between the values at pH 7 and 8.5 is not meaningful. Considering the result at pH = 3, the data indicate that the homogeneous rate increases with pH. The total rate constant k_t with cobalt sulfate added at pH = 8.5, where cobalt is an active catalyst, is about five times the result for the noncatalyzed homogeneous reaction. Since both catalytic and non-catalytic reactions are first order, the rates are additive,

$$k_t = k_h + k_{Co} \tag{29}$$

The rate constant k_{Co} for the cobalt catalyzed reaction is 0.33, s^{-1}, about four times that for non-catalyzed homogeneous rate.

Overall heterogeneous rate constant

To calculate the overall heterogeneous rate constant k_p from Eq. 18, $k_s a_s$ as well as k_t must be known. In agitated slurries of small particles, Kolmogoroff's theory (Levins and Glastonbury, 1972) relates k_s to the agitation speed and particle size. For our conditions this correlation gives 2.79×10^{-4} m/s. This value is used in Eq. 18. For comparison, the correlation proposed by Furusawa and Smith (1973) yields 2.35×10^{-4} m/s. The slope of the line in Figure 3 gives for k_o, for example at pH = 3, 1.0×10^{-3} m^3/kg · s. Using this result and the k_t (= k_h) value at pH = 3 in Eq. 12 yields the same result for k_p. This is because at our conditions the heterogeneous reaction is dominant. The value of $k_h(\beta/\rho_p)$, which according to Eq. 12 is the homogeneous contribution of the reaction in the pore liquid to the overall rate constant, is but 1% of k_o. The value of $(1 - \beta m_s/\rho_p)k_h$ is such that the homogeneous reaction in bulk liquid affects the bracketed term in Eq. 18 by a maximum of 5%. The result for k_p at pH = 2 in Table 3 was obtained by neglecting the homogeneous reaction. Operating with lower concentrations of carbon particles would have increased the relative importance of homogeneous reaction.

Adsorption and surface reaction rate constants

The first moment data at pH = 2 and 3 for the runs with carbon particles are plotted in Figure 6 as $\mu_1^o Q/V_L$ vs. $m_o(1 + 1/K_L - 1/m_o K_L)^2$. According to Eq. 21 the slope of a straight line through the data points provides the second relationship between the adsorption and surface reaction rate constants k_a and k_r (the k_o results from the zero-moment slot, Figure 3, give the first relation). Although the data are scattered in

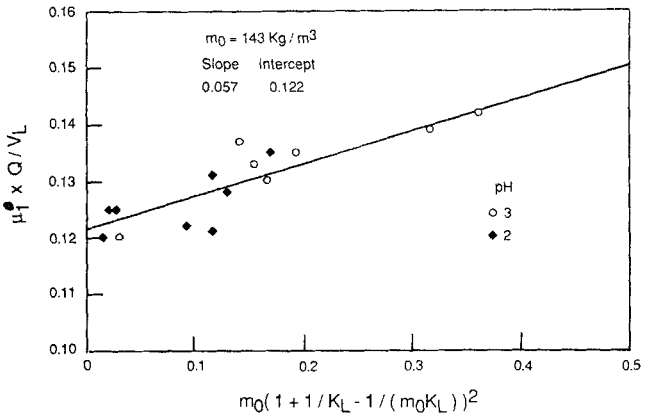

Figure 6. First moments for homogeneous plus heterogeneous reaction (pH 2 and 3).

Figure 6, an approximate straight line fit can be obtained by linear regression. No distinction can be made between the results for pH 2 and 3, so all the data were used to give the slope shown. In preparing the abscissa for this figure, K_L is given by the intercepts in Figure 3 and the zero-moment values.

Equation 21 shows that the slope in Figure 6 depends upon K. As mentioned, this quantity can be calculated from first-moments for runs at 295 K for adsorption of oxygen in distilled water. Figure 7 shows that data points and line established by regression analysis. According to Eq. 22 the slope of this line is $((1 + m_s K)/H + V_o/V_L)$. The corresponding value of K is $11. \times 10^{-3}$ m^3/kg, independent of pH between 6 and 9. Recasens et al. (1984) for the same system obtained $K = 12.4 \times 10^{-3}$ at 293 K and 10.8×10^{-3} m^3/kg at 299 K. It is assumed that the adsorption equilibrium constant for oxygen is independent of pH so that the value of $K = 11 \times 10^{-3}$ can be used for further calculations. In our evaluation of K, m_s = 136 kg/m^3 and $V_L = 1.0 \times 10^{-3}$ m^3.

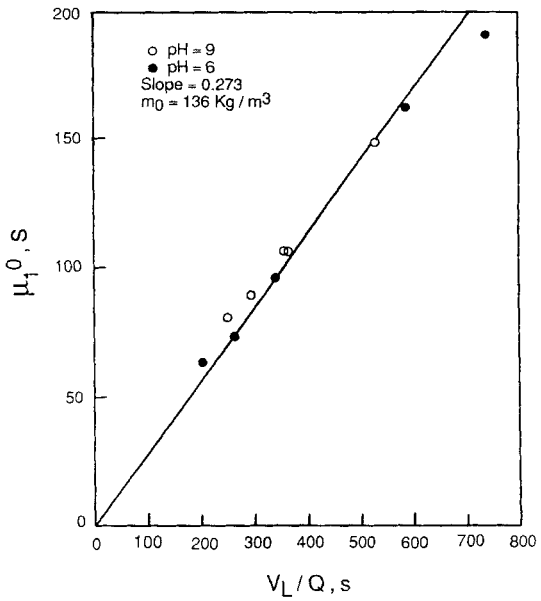

Figure 7. First moments for oxygen adsorption in aqueous slurries of activated carbon.

Table 3. Equilibrium and Kinetic Constants for Combined Homogeneous and Heterogeneous Reaction (T = 295 K)

	pH			
	2	3	7	8.5
$k_h \times 10^2$ (1/s)	—	1.0	10.	8.8
$k_o \times 10^3$ (m^3/g · s)	2.2	1.0	—	—
$k_p \times 10^3$ (m^3/kg · s)	2.2	1.0	—	—
k_r (1/s)	0.21	0.10	—	—
$k_a \times 10^2$ (m^3/kg · s)	4.6	1.1	—	—
$K \times 10^3$ (m^3/kg)	11.0	11.0	—	—
$k_r/(k_a/K)$	0.05	0.10	—	—
$k_{Co} \times 10^2$ (1/s)	—	—	—	33
$k_t \times 10^2$ (1/s)	—	—	—	42

The results for the ratio $k_r/(k_a/K)$, obtained from the slope in Figure 6, k_p, K, and k_o from the zero-moment data, are given in Table 3. This ratio is a measure of the relative importance of surface reaction and adsorption to the overall heterogeneous reaction. The low values (<1) suggest that surface reaction is the controlling step. With $k_r/(k_a/K)$ and k_p known, Eq. 13 was used to obtain the separate values of k_a and k_r tabulated in Table 3. The results of Recasens et al. (1984) gave somewhat higher values for the ratio and considerably lower results for k_a and k_r. The difference seems to be due to errors associated with the discontinuous sample analysis procedure in the work of Recasens et al., and due to the scatter in the first-moment results in both studies. Large uncertainties in k_a, particularly, are due to the difficulty in measuring accurate first moments. However, the Recasens et al. investigation gave value of $k_r/(k_a/K)$ less than unity confirming our result that surface reaction of adsorbed oxygen is the dominant step in determining the rate of the heterogeneous reaction.

Acknowledgment

Financial assistance from the University of California and Chevron Research Corporation are gratefully acknowledged.

Notation

A = strength of input pulse
a_B = surface area of gas bubbles per unit volume of bubble-free liquid, m^2/m^3
a_s = surface area of catalyst particle per unit volume of bubble- and particle-free liquid, m^2/m^3
B_o = dimensionless group defined in Eq. 14
B_s = dimensionless group defined in Eq. 10
C_g = gas concentration in bubbles, gmol/m^3, C_{go} = gas concentration in feed
$\bar{C}_g$ = Laplace transform of C_g
C_L = gas concentration in bulk liquid, gmol/m^3
H = Henry's law constant, C_g/C_L
k_a = adsorption rate constant for the heterogeneous reaction, m/kg · s
$k_t \equiv k_h + k_{Co}$, rate constant for the total homogeneous reaction, 1/s
k_{Co} = rate constant for the cobalt catalyzed homogeneous reaction, 1/s
k_h = reaction rate constant for the noncatalyzed homogeneous reaction, 1/s
k_L = gas bubble-to-liquid mass transfer coefficient, m/s
k_p = overall reaction rate constant for the heterogeneous reaction, m^3/kg · s
k_r = surface reaction rate constant for the heterogeneous reaction, 1/s
k_o = combined reaction rate constant defined in Eq. 12, m^3/kg · s
k_s = liquid-to-solid mass transfer coefficient, m/s
K_L = dimensionless mass-transfer parameter defined in Eq. 15
K = adsorption equilibrium constant, m^3/kg
m_o = zero moment
m_1 = first moment, s
m_n = nth moment, s^n
m_s = mass of heterogeneous catalyst particles per unit volume of bubble- and particle-free liquid, kg/m^3
n = concentration of gas adsorbed on heterogeneous catalyst particles, gmol/m^3
P = pressure, atm
Q = volumetric gas flow rate, m^3/s
R = radius of solid catalyst particle (spherical), m
$[SO_2]$, $[SO_3^-]$, $[HSO_3^-]$ = liquid concentrations, kmol/m^3
s = Laplace variable, s^{-1}
t = time, s
V_B = bubble volume per unit volume of bubble- and particle-free liquid
V_d = dead volume, including gas space over liquid and in tubing, m^3
V_L = volume of liquid, m^3
V_o = dead volume with no gas flow, m^3
x = conversion

Greek letters

β = porosity of catalyst particles
μ_1^o = observed reduced first moment, s
ϵ = dimensional group defined in Eq. 11
ρ_p = density of catalyst particle, kg/m^3

Literature Cited

Ahn, B.-J., J. M. Smith, and B. J. McCoy, "Dynamic Hydrogenation Studies in a Catalytic Slurry Reactor," *AIChE J.*, **32**, 566 (Apr., 1986).

Boyce, S. D., M. R. Hoffman, P. A. Hong and L. M. Moberly, "Meterorological Aspects of Acid Rain," ed., C. M. Bhumralkar, Ch. 11, 163 (1984).

Chang, S. G., D. Littlejohn, and K. Y. Hu, "Disulfate Ion as an Intermediate to Sulfuric Acid in Acid Rain Formation," *Sci.*, **237**, 756 (1987).

Chaudhari, R. V., and P. A. Ramachandran, "Three Phase Slurry Reactors," *AIChE J.*, **26**, 177 (Apr., 1980).

Fu, C.-C., J. M. Smith, and B. J. McCoy, "Dynamic Analysis of Homogeneous Reactions in a Stirred Bubble Reactor: Oxidation of Sulfite," *Chem. Eng. Sci.*, **43**, 1231 (1988).

Fu, C.-C., Ph.D. Diss., Univ. of California, Davis (1988).

Furusawa, T., and J. M. Smith, "Fluid-Particle and Intraparticle Mass Transfer Rates in Slurries," *Ind. Eng. Chem. Fund.*, **12**, 197 (1973).

Gould, E. S., and M. Rado, "Homogeneous vs. Heterogeneous Catalysis: Oxidation of Liquid Cyclohexene Catalyzed by Ions and Oxides of Transition Metals," *J. of Cat.*, **13**, 238 (1969).

Hartman, M., J. R. Polek, and R. W. Coughlin, "Removal of Sulfur Dioxide from Fuel Gas by Sorption and Catalytic Reaction on Carbon," *AIChE Symp. Ser.*, **7**, No. 115, 7 (1971).

Kaul, D. J., R. Sant, and E. E. Wolf, "Integrated Kinetic Modelling and Transient FTIR Studies of CO_2 Oxidation on Pt/SiO_2," *Chem. Eng. Sci.*, **42**, 1399 (1987).

Komiyama, H., and J. M. Smith, "Sulfur Dioxide Oxidation in Slurries of Activated Carbon," *AIChE J.*, **21**, 664 (Aug., 1975).

Levins, D. M., and J. R. Glastonbury, "Application of Kolmogoroff's Theory to Particle-Liquid Mass Transfer in Agitated Vessels," *Chem. Eng. Sci.*, **27**, 537 (1972).

Misic, D., and J. M. Smith, "Adsorption of Benzene in Carbon Slurries," *Ind. Eng. Chem. Fund.*, **10**, 380 (1971).

Muller, E., and H. Hofmann, "Dynamic Modelling of Heterogeneous Catalytic Reactions: I. Theoretical Considerations," *Chem. Eng. Sci.*, **42**, 1695 (1987a), II. Experimental Results—Oxydehydrogenation of Isobutyric Aldehyde to Methacrolein," *ibid.*, 1705 (1987b).

Newberg, H. J., J. M. Basset, and W. F. Graydon, "Heterogeneous Liquid-base Oxidation of Cyclohexene with Manganese Dioxide as Catalyst," *J. of Cat.*, **25**, 425 (1972).

Recasens, F., J. M. Smith, and B. J. McCoy, "Temperature Effects on Separate Values of Adsorption and Surface Reaction Rates by Dynamic Studies," *Chem. Eng. Sci.*, **39**, 1469 (1984).
Skoog, D. A., and D. M. West, "Fundamentals of Analytical Chemistry," 3rd Ed., Holt, Rinehart and Winston, New York, 785 (1976).
Taylor, W. F., "Catalysis in liquid-phase Autoxidation, I. Effect of Polymeric Surfaces," *J. of Cat.*, **16**, 20 (1970).
van Krevelen, D. W., and P. J. Hoftijzer, *Chimie et Industrie: Numero Speciale du XXI Congress Internationale de Chimie Industrielle*, Briuxelles, 168 (1948).
Vreugdenhil, A. D., "Mechanism of the Silver-on-silica Catalyzed Oxidation of Cumene in the Liquid Phase," *J. of Cat.*, **28**, 493 (1973).
de Waal, K. J. A., and J. C. Okeson, "The Oxidation of Aqueous Sodium Sulfite Solutions," *Chem. Eng. Sci.*, **21**, 559 (1966).
Yagi, S., and H. Inoue, "The Absorption of Oxygen into Sodium Sulphite Solution," *Chem. Eng. Sci.*, **17**, 411 (1962).

Manuscript received Mar. 2, 1988, and revision received Sept. 13, 1988.